Assessing Accumulated Solvent Near a Macromolecular Solute by Preferential Interaction Coefficients

Karen E. S. Tang and Victor A. Bloomfield
Department of Biochemistry, Molecular Biology, and Biophysics, University of Minnesota, Saint Paul, Minnesota 55108-1022 USA

ABSTRACT Biological macromolecules are often studied in mixed solvents. To understand cosolvent-macromolecule interactions, the preferential interaction coefficient, Γ_3, may help determine surface solvent compositions. Γ_3 measures the amounts of water, B_1, and cosolvent, B_3, within the "local domain," the (possibly far-reaching) region surrounding the macromolecule where the solvent is nonbulk-like. The local domain's boundary is, however, vague and it is unclear which molecules are counted in B_i. It is useful to explore a simple model system to make B_i more concrete and to understand which aspects of the surface solvent distribution, $\rho(x)$, are sampled by Γ_3. We performed computer simulations on a two-dimensional (2D) system consisting of a hard-wall solute (the macromolecule) in a mixed solvent (hard disks of different radii). We simultaneously calculated Γ_3 and $\rho(x)$. We found that 1) in practice, the local domain's boundary is demarked by the outer limit of the first cosolvent (not water) layer; B_i mainly counts the solvent near the macromolecule; 2) assuming B_1 to count only the waters within the first water layer is a poor approximation; 3) when determining B_1 and B_3, water and cosolvent molecules must be counted from the same region of space. We speculate that these 2D results may serve as a first-order approximation for the dominant contributions to Γ_3 even in three dimensions, so long as the cosolvent is not strongly excluded from the macromolecular surface and there is no significant long-ranged solvent structure.

INTRODUCTION

Mixed solvent systems are important to the understanding of the structure and stabilities of macromolecules. For example, the cosolvents urea and guanidine hydrochloride have long been used to study protein denaturation, sucrose is added to stabilize proteins, and alcohols are condensing agents for DNA. (Technically, molecules such as urea, guanidine hydrochloride, and sucrose are cosolutes. However, at typical concentrations, they make up a significant fraction of the solution—8M urea is 43 wt % urea and 2 M sucrose is 55 wt % sucrose. These cosolute molecules bathe and solvate the macromolecular solute as water does. To emphasize the cosolvents' role in solvation and to treat them on an equal footing with water, we refer to both cosolvents and cosolutes as "cosolvent" molecules.)

To understand cosolvent-macromolecule interactions, it is necessary to determine where the cosolvent molecules are; do they tend to lie within the bulk solvent or do they prefer to associate with the macromolecule? In particular, what is the distribution (or the composition) of solvent at the macromolecular surface? Currently, there is little information on this. The primary experimental means of obtaining atomic-resolution data on solvent structure are x-ray diffraction and nuclear magnetic resonance (NMR) experiments (Wiithrich et al., 1996). Both types of experiments are fairly complex and require specialized equipment. Also, they tend not to see all solvent molecules equally. Crystallography detects the more ordered waters (Levitt and Park, 1993) whereas NMR more easily sees those with longer residence times and those that are closer to the surface (Otting et al., 1991; Otting, 1997). (In several NMR studies of proteins in mixed solvents, only a few cosolvent molecules could be unambiguously identified (Liepinsh and Otting, 1997; Ponstingl and Otting, 1997; Liepinsh et al., 1999).) Other techniques, such as hydrodynamic, small-angle x-ray and neutron scattering, calorimetric, dielectric, and vapor-pressure absorption isotherm experiments, provide only low-resolution data on surface-associated solvent (see, e.g., Kuntz and Kauzmann, 1974; Pessen and Kumosinsky, 1985; Rupley and Careri, 1991; Svergun et al., 1998). Atomic-resolution molecular mechanics simulations pose as an alternative to experiment; in practice, however, equilibrating the mixed solvent in the presence of a macromolecule is time-consuming and, to date, only two works (Tirado-Rives et al., 1997; Sprous et al., 1998) have published the distributions of neutral cosolvents at a macromolecular surface.

Measurement of the preferential interaction coefficient, Γ_3,

$$\Gamma_3 \equiv \frac{\partial m_3}{\partial m_2} \tag{1}$$

is a potentially powerful tool for examining the solvent at a macromolecular surface. (We use the following notation: component 1 is water, 2 is the macromolecular solute, which we sometimes refer to simply as the "solute," and 3 is the cosolvent. We use the term "solvent" to mean the mixed solvent, not water; m_i is the molality of species i.)

Submitted July 2, 2001 and accepted for publication March 18, 2002.

Address reprint requests to Dr. Victor A. Bloomfield, Dept. of Biochemistry, 140 Gortner Lab, University of Minnesota, 1479 Gortner Ave., St. Paul, MN 55108. Tel.: 612-625-2268; Fax: 612-625-5780; E-mail: victor.a.bloomfield-1@tc.umn.edu.

0006-3495/02/06/2876/16 $2.00

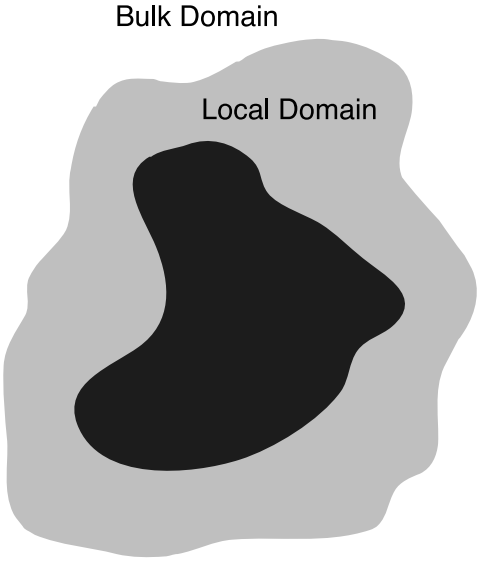

FIGURE 1 The two-domain model. The "bulk domain" is the region where the solvent has characteristics of bulk solvent, as if there were no solute present. The solvent in the "local domain" is in some way altered by the presence of the solute. There is no well-defined boundary between the local and the bulk domains (Kuntz and Kauzmann, 1974).

Experiments to measure Γ_3 are straightforward (although tedious) and can be done by a variety of methods (see, e.g., Casassa and Eisenberg, 1964; Kuntz and Kauzmann, 1974; Eisenberg, 1976; Schellman, 1990; Timasheff, 1993, 1998; Zhang et al., 1996; and references therein). Many Γ_3 data have already been gathered on proteins and DNA in the presence of many cosolvents as discussed in several review articles (Kuntz and Kauzmann, 1974; Timasheff, 1993, 1998).

To understand what Γ_3 tells us about the water and cosolvent distributions (or compositions) at a solute surface, let us first describe in molecular terms what Γ_3 measures by using the "local-bulk domain" (AKA "two-domain") model (see Record et al., 1998 and references therein), depicted in Fig. 1. The "bulk domain" consists of the region where the solvent displays the same properties as the mixed solvent in the absence of macromolecular solutes. That region is sufficiently far away from any solute so that the solvent doesn't "know" anything about the presence of solutes. In the "local domain" the solvent properties have in some way been affected by the solute. When all species are uncharged and when Γ_3 is measured at dilute concentration of solute, Γ_3 can be interpreted as (Record and Anderson, 1995; Inoue and Timasheff, 1972; Reisler et al., 1977)

$$\lim_{m_2 \to 0} \Gamma_3 = B_3 - \frac{m_3^{bulk}}{m_1} B_1 \qquad (2)$$

where B_i is the number of i molecules (per solute) in the local domain (i = water or cosolvent; m_3^{bulk} is the cosolvent molality of the mixed solvent in the absence of solute; m_1 is a constant, equal to 55.5 mol/kg for water). Record and Anderson (1995) put this equation on a more rigorous footing by showing that it is exact for the common situation of measurement of Γ_3 by dialysis equilibrium even when m_2 is not negligibly small. (They also proposed functional forms for how B_3 and B_1 depend on m_3^{bulk}, in terms of coefficients of partition and stoichiometry of solvent-cosolvent exchange. However, representation in terms of these coefficients is not necessarily unique.) It is not necessary to make any assumptions regarding the nature of the interaction between either solvent species and the solute (Na and Timasheff, 1981); the interactions can be attractive or repulsive or the solute may merely change the structure of the mixed solvent such that the local density of either or both solvent species is altered. One can also write for the preferential hydration, $\Gamma_1 = -(m_1/m_3^{bulk})\,\Gamma_3$ (see Schellman, 1990 and references therein),

$$\lim_{m_2 \to 0} \Gamma_1 = B_1 - \frac{m_1}{m_3^{bulk}} B_3. \qquad (3)$$

Γ_1 is merely a different way of presenting the information in Γ_3. In this work we consider only uncharged species. The equations for Γ_3 and Γ_1 are modified when charges are present (see, e.g., Record et al., 1998).

(Note that in the literature there is another valid interpretation of Eqs. 2 and 3, in which the B_i values are heuristically thought of as "effective total numbers of [cosolvent] and water molecules in contact with sites on the [solute] surface" (Timasheff, 1998). The exact interpretation used here and by others (Arakawa and Timasheff, 1982b; Record and Anderson, 1995; Hammou et al., 1998) is different in that the B_i values count the number of real solvent molecules in the entire local domain, not solvent molecules effectively contacting the solute surface.)

The sign of Γ_3 tells us about the local solvent composition as compared to that of the bulk solvent. Dividing Eq. 2 by B_1 (which is positive by definition), we see that the sign of Γ_3 is determined by the quantity $B_3/B_1 - m_3^{bulk}/m_1$. B_3/B_1 and m_3^{bulk}/m_1 are the cosolvent:water number ratios in the local domain and of the bulk binary solvent, respectively. When $\Gamma_3 < 0$ ($\Gamma_1 > 0$), the solvent composition (but not necessarily the solvent density) of the local domain is depleted in cosolvent and/or enriched in water relative to that of the bulk binary solvent. This is what is meant by the term "preferential hydration." Likewise, when $\Gamma_3 > 0$ ($\Gamma_1 < 0$) the solvent composition of the local domain is depleted in water and/or enriched in cosolvent relative to bulk, and is described by the term "preferential binding" (although there may be no actual binding going on) or "preferential accumulation" of cosolvent. "Preferential solvation" by water/cosolvent is another commonly used term.

Unfortunately, it is not yet clear how to interpret the magnitude of Γ_3. Because solvent interactions are relatively weak, there is unlikely to be a sharp physical boundary between the local and bulk domains (Kuntz and Kauzmann, 1974). Hence, one cannot say definitively which solvent molecules are counted in B_i and contributing to Γ_3. Also, for the purpose of understanding solute-solvent interactions, information on the solvent population right next to the solute is desired. However, experimental evidence indicates that the local domain can extend over quite a large territory, even when the interactions are short-ranged. For example, changes in water structure due to solid hydrophobic surfaces can be sensed tens of nanometers away (see, e.g., Blokzijl and Engberts, 1993; Vogler, 1998). Even the water distribution around proteins (Komeiji et al., 1993; Lounnas et al., 1994; Makarov et al., 1998), peptides (Gerstein and Lynden-Bell, 1993), and small solutes (e.g., argon (Blokzijl and Engberts, 1993) and *N*-methylacetamide (Beglov and Roux, 1996)) as well as the distributions of urea and trifluoroethanol around a methane solute (Smith, 1999) display two or more peaks, corresponding to two or more layers of structured solvent. Thermodynamic experiments suggest that the protein perturbs solvent beyond the first water shell (see Lounnas et al., 1994 and references therein). In summary, not only is it not clear which solvent molecules are counted in B_i, but also the counted solvent molecules may not be contacting, nor binding, nor necessarily even close to the solute. Because of these two issues, it is not yet clear how to turn Γ_3 data into quantitative information on the solvent population near the solute.

The broad goal of our research is to get quantitative information on the solvent distribution (or composition) at the solute surface from Γ_3. In particular, we would like to obtain the number of cosolvent (water) molecules within the first cosolvent (water) shell at the solute surface. We call this quantity $B_3^{fs}(B_1^{fs})$, "*fs*" standing for first shell. To obtain B_1^{fs} and B_3^{fs} from Γ_3 and B_i data two hurdles need to be overcome.

The first hurdle is that the relationship between B_i^{fs} and B_i needs to be determined. The latter measures the number of *i*'s in the entire local domain, which clearly encompasses *i*'s first shell but likely extends further (i.e., $B_i \geq B_i^{fs}$). However, in practice, because the solvent molecules that are most affected by the solute lie close to it, one expects that the major contribution to Γ_3 should be due to the first-shell solvent molecules. If Γ_3 is mostly a function of the B_i^{fs} values, then B_i should in some way also be dominated by B_i^{fs}. However, this relationship between B_i and B_i^{fs} has not yet been worked out. Another way to phrase the issue is that the exact definition of B_i is not very useful for understanding solvent behavior near a solute, as B_i counts the solvent over a poorly demarked and potentially large territory. Can we find an approximate definition of B_i based on the nearby solvent distribution that, when plugged into Eq. 2, gives a good first-order approximation to Γ_3? If so, then we can get a sense of how Γ_3 samples the properties of the nearby solvent distribution.

Second, a validated method of obtaining B_1 and B_3 from Γ_3 is needed. With one experimental quantity (Γ_3) and two desired unknowns (B_1 and B_3), some assumptions on the B_i values or on the solvent distributions must be made. For example, 1) it has been suggested that B_1 be obtained from (or compared to) independent experiments on the macromolecular solute in the absence of cosolvent (Inoue and Timasheff, 1972; Lee and Timasheff, 1974, 1981; Lee and Lee, 1981; Na and Timasheff, 1981; Arakawa and Timasheff, 1982a, b, 1985; Timasheff, 1998; Courtenay et al., 2000a), e.g., by the NMR method of Kuntz (1971) or by the vapor pressure measurements of Bull and Breese (1968), or that B_1 be obtained using a different cosolvent (e.g., a "completely excluded" one (Courtenay et al., 2000a)). The assumption here is that B_1 is unchanged by the addition of (or a change in the) cosolvent. 2) Various researchers have made comparisons of B_1 values to the amount of water in a monolayer (Zhang et al., 1996; Hammou et al., 1998; Courtenay et al., 2000a) suggesting that $B_1 \sim B_1^{fs}$ and that the local domain extends only through the first shell of the water, the mixed solvent further out behaving (mostly) like bulk. 3) To explain the effects of denaturants on proteins, it has been assumed that the cosolvent partition coefficient and water-cosolvent exchange stoichiometry are independent of cosolvent concentration (Courtenay et al., 2000b). 4) A steric-exclusion model (Arakawa and Timasheff, 1985; Bhat and Timasheff, 1992) attributes preferential hydration to the cosolvent molecules' larger-than-water size. The cosolvent molecules cannot closely approach the solute, and the region right up against the solute is assumed to be filled only with pure bulk water. 5) In the analysis of osmotic stress experiments, which often aim to measure the number of water molecules "bound" or "released" in a reaction like the binding of a ligand to a protein (Parsegian et al., 1995), it is assumed that $\Delta B_3 = 0$ (see Parsegian et al., 1995; Timasheff, 1998, references therein, and below). Parsegian et al. (1995) discuss under what conditions this approximation is valid, but not all works have followed their careful guidelines. (To translate the language of osmotic stress to that of preferential interactions, see Table 1 of Parsegian et al., 2000; also, what is called N_{ew}, the "excess number of waters," is equivalent to Γ_1; similarly, N_{es}, the "excess number of [cosolvent molecules]," is Γ_3. By equating ΔN_{ew} with a difference in number of waters associated with the product versus with the reactant, the implicit assumption is that $\Delta B_3 = 0$.) 6) By assuming that B_1 and B_3 values are constant, independent of solvent composition, the B_i values can be readily obtained from the slope and intercept of linear Γ_3 versus m_3^{bulk} (or Γ_1 versus $1/m_3^{bulk}$) plots (Reisler et

TABLE 1 Simulation details

R_3/R_1	r_3^{bulk}	Cos:Wat "Volume" Ratio*	Box Dimensions†	Γ_3‡
1.3	0.5847	0.99	28.0 × 28.5	−0.00842 ± 2.9%
1.3	0.2953	0.50	28.0 × 42.6	−0.00571 ± 2.4%
1.6	0.5825	1.50	28.0 × 35.8	−0.0135 ± 1.2%
1.6	0.3867	0.99	28.0 × 71.8	−0.0110 ± 1.1%
1.6	0.2941	0.75	28.0 × 49.9	−0.0099 ± 1.2%
1.6	0.1927	0.49	28.0 × 64.7	−0.072 ± 1.6%
2.0	0.2463	0.99	40.0 × 47.1	−0.0118 ± 1.5%
2.0	0.1641	0.66	40.0 × 49.1	−0.00937 ± 1.9%
2.0	0.1232	0.49	40.0 × 47.1	−0.00813 ± 2.2%
2.0	0.08210	0.33	40.0 × 47.1	−0.00584 ± 4.0%
2.0	0.06211	0.25	40.0 × 58.9	−0.00460 ± 2.7%
2.0	0.03070	0.12	40.0 × 106	−0.00257 ± 6.7%
2.0	0.01539	0.062	40.0 × 200	−0.00140 ± 3.9%
2.0	0.007692	0.031	40.0 × 389	−0.00068 ± 7.2%
2.3	0.1853	0.98	28.0 × 89.1	−0.0117 ± 1.2%
2.3	0.09251	0.49	28.0 × 89.1	−0.0077 ± 1.5%
3.0	0.1084	0.98	40.0 × 70.7	−0.0103 ± 3.6%
3.0	0.07270	0.65	40.0 × 70.7	−0.0087 ± 6.0%
3.0	0.05462	0.49	40.0 × 79.5	−0.0074 ± 8.1%
3.0	0.03609	0.32	40.0 × 106	−0.0056 ± 7.5%
3.0	0.02720	0.24	28.0 × 189	−0.0044 ± 8.0%
3.0	0.01363	0.12	28.0 × 341	−0.0024 ± 4.8%
3.0	0.009092	0.082	28.0 × 492	−0.0016 ± 7.0%
4.0	0.05991	0.96	32.0 × 157	−0.076 ± 10.5%

In addition to the binary solvents listed here, available from the authors are data with $\eta = 0.33$, $R_3/R_1 = 1.26$, 2.0, 3.0, and 4.0, and $\eta = 0.5$, $R_3/R_1 = 2.0$. Most of the simulations were run with 1.5×10^9 trial moves, 0.5×10^9 of them during the equilibration phase; the only exceptions were the systems ($R_3/R_1 = 2.3$, $r_3^{bulk} = 0.1853$ and 0.09251: 3.0×10^9 total trial moves, 0.25×10^9 equilibration); ($R_3/R_1 = 3.0$, $r_1^{fs} = 0.1084$: 1.4×10^9 total trial moves, 0.4×10^9 equilibration); ($R_3/R_1 = 3.0$, $r_3^{bulk} = 0.02720$; 6.0×10^9 total trial moves, 0.5×10^9 equilibration); ($R_3/R_1 = 3.0$, $r_3^{bulk} = 0.01363$: 24×10^9 total trial moves, 0.5×10^9 equilibration); ($R_3/R_1 = 3.0$, $r_3^{bulk} = 0.009092$: 24×10^9 total trial moves, 1.0×10^9 equilibration); and ($R_3/R_1 = 4.0$, $r_3^{bulk} = 0.05991$: 2.0×10^9 total trial moves, 1.0×10^9 equilibration).

*The ratio of the total 2D volume occupied by cosolvent relative to the total volume occupied by water, $(\langle N_3^{bulk}\rangle \pi R_3^2)/(\langle N_1^{bulk}\rangle \pi R_1^2)$.

†In units of R_1. Both the ms box and the bulk box are the same dimensions, listed as the distance between the hard walls × the length of the hard wall.

‡Per unit length of hard wall.

al., 1977; Lee and Lee, 1979, 1981; Na and Timasheff, 1981; Lee and Timasheff, 1981; Eisenberg, 1994).

Clearly, various assumptions have been used to understand Γ_3 (or Γ_1) data or to extract B_1 and B_3 values from these data; to date, none of these assumptions has been validated against surface solvent distributions.

To overcome these two hurdles, what is needed is a way to measure, on the same solute-mixed solvent system, both Γ_3 and the water and cosolvent distributions around the solute. From the latter, B_i and B_i^{fs} values can be calculated. As discussed above, obtaining solvent distribution data on mixed solvents from either experiment or from atomic-resolution simulations is difficult. We therefore turn to modeling simple systems. In this work, we have performed Monte Carlo simulations on two-dimensional (2D) systems consisting of a 2D "box" with two hard "walls"; the box contains a binary mixture of small (component 1) and large (component 3) circular hard disks (see the sample configuration in Fig. 2 A). The hard wall mimics a macromolecular surface (component 2). The small and large hard disks are simplified representations of the water and cosolvent molecules, respectively. The number and size ratios of the small-to-large disks are varied to study different solvent compositions and cosolvents of different sizes. Because of the absence of directed soft interactions, we can investigate excluded-volume contributions to Γ_3. We chose to model a 2D system because the lower dimensionality lets us simulate a system with many fewer molecules (a ratio of $\sim N^{-1/3}$ fewer than in three dimensions) with a considerable savings in computational time. This is critical because it is difficult to gather sufficient statistics to precisely determine Γ_3 (which is a measure of fluctuations). The time savings allows us to examine many different water:cosolvent compositions—including those fairly dilute in cosolvent—and several different cosolvent sizes. Equilibration was not a serious issue (as it is for more realistic simulations) except in cases of very dilute cosolvent and/or large cosolvent molecules. Because our conclusions are qualitative, originating from a sound physical basis, extending our results to three dimensions and to complex-shaped molecules is straightforward.

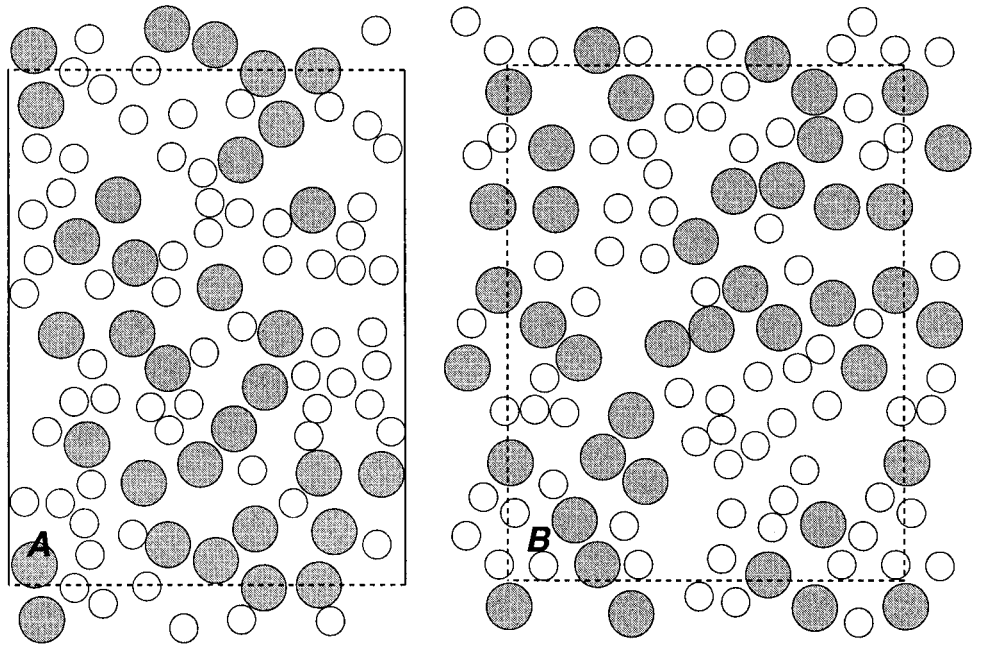

FIGURE 2 Sample configurations of the ms (*A*) and the bulk (*B*) boxes. The *small light gray circles* represent the water molecules, the *large dark gray circles* the cosolvent molecules. The dotted box boundaries represent the periodic boundary conditions, and the solid boundaries the hard walls. Here, $R_3/R_1 = 1.6$ and $r_3^{\text{bulk}} = 0.5825$.

For each of the many solvent compositions and cosolvents we studied, we analyzed the surface solvent distributions and made comparisons to Γ_3. We found the following: 1) although the local domain in principle can extend quite far from the solute surface, in practice, its boundary can be demarked by a cosolvent (not water) monolayer, if solvent structure is short-ranged. (The cosolvent monolayer is thicker than the water monolayer because cosolvent molecules are larger than water molecules.) 2) The solvent structure associated with the second and further layers of solvent can mostly be ignored (if solvent structure is short-ranged). 3) Combining 1) and 2) yields a recipe for B_i (see also Fig. 3 *B*):

$$B_1 \sim B_1^{\text{fs}} + \rho_1^{\text{bulk}} (V_3^{\text{fs}} - V_1^{\text{fs}}) \quad (4)$$

$$B_3 \sim B_3^{\text{fs}} \quad (5)$$

where ρ_1^{bulk} is the average water number density in the bulk mixed solvent, and $(V_3^{\text{fs}} - V_1^{\text{fs}})$ is the difference between the volume of space corresponding to the cosolvent first shell (V_3^{fs}) and that corresponding to the water first shell (V_1^{fs}). $\rho_1^{\text{bulk}} (V_3^{\text{fs}} - V_1^{\text{fs}})$ is the amount of water that would be in the region of space between the end of the water first shell and the end of the cosolvent first shell if it were filled with bulk mixed solvent. 4) Including only first-shell waters in B_1 is not a good approximation ($B_1 \not\sim B_1^{\text{fs}}$). These results are, of course, specific to the simple 2D solvent/solute system we studied. However, because the main assumption behind these conclusions is that the degree of solute-induced solvent structure associated with the first cosolvent shell is much larger than that associated with the second and further shells (and likewise for water), these results may serve as a first-order approximation for real solvents whenever the solvent-structure induced by the solute is short-ranged and neither solvent species is strongly repelled by the solute. Lastly, we also investigated a steric-exclusion model of preferential hydration (Arakawa and Timasheff, 1985; Bhat and Timasheff, 1992). The model's approximations on the solvent distribution are nonphysical and the predictions of Γ_1 values are not accurate.

METHODS

Model of the solvent and solute

In our simplified model, the water and cosolvent are small and large hard circular 2D disks of radii R_1 and R_3, respectively. The macromolecular solute's surface is modeled as a flat hard 2D "wall" of effectively infinite length. The only interactions are excluded-volume in nature. The solvent molecule disks cannot overlap with each other or with the solute hard wall. Fig 2 *A* displays a sample configuration.

We chose to model this simple system primarily for the savings in computational time, as mentioned in the Introduction. Representing the solvent and solute as low-resolution hard circular disks and as a hard flat surface, respectively, also speeds computation and allows us to examine excluded-volume effects on Γ_3 without the complication of shape effects. Future work would involve simulations of the hard sphere model in three dimensions to make direct comparisons with experiment, and might also

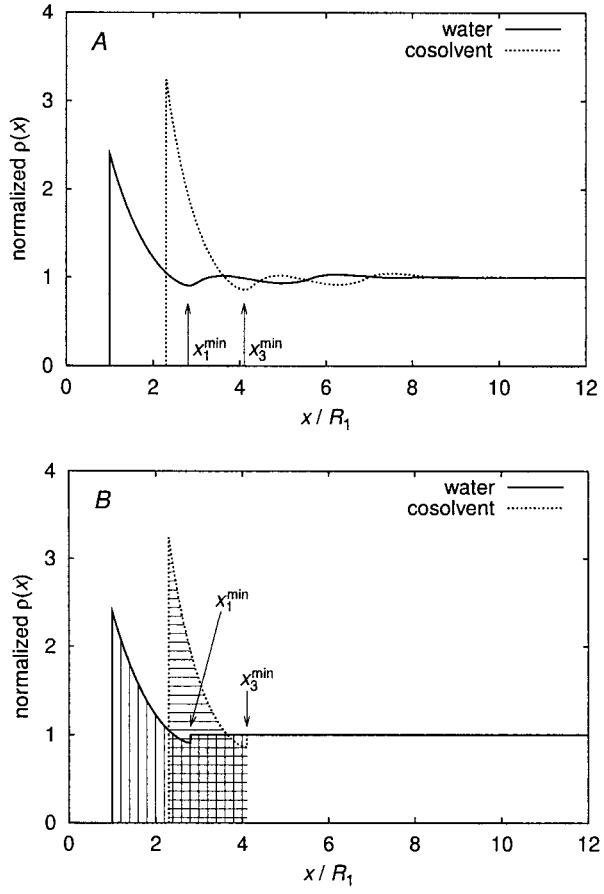

FIGURE 3 (A) Sample $\rho(x)$ data, normalized by the bulk density in the mixed solvent. This distribution is typical in that there is an unambiguous, large first peak corresponding to the first layer of solvent, and often several smaller peaks corresponding to the second and further layers. In this example, $R_3/R_1 = 2.3$ and $r_3^{bulk} = 0.1853$. (*B*) Approximated $\rho(x)$, same as *A* with the bumps and wiggles associated with the second and further layers of solvent flattened to bulk densities. For this approximate surface solvent distribution, the local domain's outer boundary is at x_3^{min}. Therefore, B_i counts the number of solvent molecules out to x_3^{min}. B_1 and B_3 are represented by the vertically and horizontally hatched regions, respectively.

add soft interactions (see, e.g., Silverstein et al., 1998) and examining differently shaped solutes and solvent.

In this work we performed simulations with several different cosolvent radii: $R_3/R_1 = 1.3$ (which is approximately the cosolvent:water hard-sphere-radius ratio for methanol); 1.6 (ethanol, ethylene glycol, trifluoroethanol, urea); 2.0, 2.3 (glucose); 3.0 (sucrose); and 4.0 (which is the ratio of the radius of gyration of PEG 200 to the water radius). To obtain the values of R_3/R_1, the hard-sphere radii are averages from values tabulated in Tang and Bloomfield, 2000, except that of trifluoroethanol is an average from the values calculated using the methods described in Edward, 1970 and Ben-Amotz and Willis, 1993, and the radius of gyration of PEG 200 is from Bhat and Timasheff, 1992.

Monte Carlo simulations

We mimic a dialysis equilibrium by simulating two different boxes, one (denoted the "ms" box) containing the hard-wall macromolecular solute surface plus binary solvent; and the other box ("bulk"), containing only the binary solvent. Fig. 2, *A* and *B* show sample configurations of the ms and bulk boxes, respectively. Each box, separately, is simulated under the grand canonical ensemble with the parameters (μ_1, μ_3, V). This means that the water and the cosolvent in the ms box are in chemical equilibrium with the water and the cosolvent of an infinite bath of mixed solvent with parameters (μ_1, μ_3); the bulk box's solvent is also in exchange equilibrium with an infinite bath of mixed solvent with the same parameters (μ_1, μ_3). Because the solvent of both the ms and bulk boxes are in chemical equilibrium with the same infinite mixed-solvent bath, the ms and bulk boxes are, in effect, in chemical equilibrium with each other. This is how we mimicked a dialysis equilibrium.

Because both boxes (separately) were simulated under the grand canonical ensemble, the numbers of water and cosolvent molecules (N_1 and N_3, respectively) in each box fluctuate, but their equilibrium averages $\langle N_1\rangle$ and $\langle N_3\rangle$ are well defined. Because of the constraint of not allowing overlap of solvent with the hard walls, there is a very small net reduction of particles from the ms box relative to the bulk box ($\langle N^{ms}{}_i\rangle < \langle N^{bulk}{}_i\rangle$), which is what Γ_3 detects.

In this paper we examine many different binary solvents, each specified by the variables (R_3/R_1, r_3^{bulk}, η), where r_3^{bulk} is the average cosolvent:water number ratio in the bulk binary solvent ($r_3^{bulk} \equiv \langle N_3^{bulk}\rangle/\langle N_1^{bulk}\rangle = m_3^{bulk}/m_1$), and η is the average packing fraction (fractional volume occupancy) of the bulk solution ($\eta \equiv (\langle N_3^{bulk}\rangle\pi {R_3}^2 + \langle N_1^{bulk}\rangle\pi {R_1}^2)/V$). Except where indicated, all studies were performed with $\eta = 0.39-0.40$. We chose this value because, at this density, the amount of surface solvent structure is as much as or more than that seen by experiment and high-resolution simulations (see, e.g., Burling et al., 1996; Tirado-Rives et al., 1997; Sprous et al., 1998; Pettitt et al., 1998). In any case, changing the overall packing fraction does not greatly affect the Γ_3 values. For the solvent system of ($R_3/R_1 = 2$, $r_3^{bulk} = 0.12$) reducing the packing fraction to 0.33 reduces the magnitude of Γ_3 by 14%; increasing η to 0.5 increases $|\Gamma_3|$ by 17%. For the solvent sytem of ($R_3/R_1 = 2$, $r_3^{bulk} = 0.25$), the changes in $|\Gamma_3|$ are -11% and $+7\%$, respectively.

Below, we describe the details of the boxes and the simulations. Table 1 lists the simulation parameters for each of the mixed solvents. The ms box has two opposing hard walls at left and right, and periodic boundary conditions at top and bottom. The opposing hard walls are sufficiently far apart that they are separated by a large region of solvent that is bulk-like (i.e., whose density is uniform at the same value as in the bulk box). The opposing hard walls are thus not interacting with each other and the limit of dilute solute is maintained. In the bulk box we have implemented periodic boundary conditions in all directions. Starting configurations were created by one by one, placing each solvent molecule at a random location; if there was an overlap, a new random location was selected repeatedly until a nonoverlapping location for the molecule was found. The starting values of N_i were the same for both the ms and bulk boxes.

The Monte Carlo moves for each solvent species, *i*, consisted of 1) displace steps, in which a random molecule of species *i* is displaced to a new location; the new location is random within a square with sides of length $2R_1$ centered at the molecule's original location; 2) create moves, in which a molecule of species *i* is created at a random location in the box; and 3) destroy moves, in which a random molecule of species *i* is removed from the box. The sequence of events during the Monte Carlo sequence is 1) a species (water or cosolvent) is chosen randomly; 2) a type of move (displace, create, or destroy) is chosen randomly; 3) the move is accepted or rejected based on a Metropolis criterion (see, e.g., Allen and Tildesley, 1987). In practice, because there are only hard interactions, the displace move is accepted as long as there is no overlap. The acceptance probability for the create move is $\min[1, z_i V/(N_i^{old} + 1)]$, where z_i is the activity of species *i* and N_i^{old} is the number of *i*'s in the box before the move is attempted. $z_i \equiv \exp(\mu_i/(kT))/\lambda_i^3$ (λ_i is the thermal de Broglie wavelength $\lambda_i = (h^2/2\pi m_i kT)^{1/2}$). The acceptance probability for the destroy move is $\min[1, N_i^{old}/z_i V]$. 4) The move is performed. In the case of displace and

create moves, if there is an overlap, the move is rejected. Checking for overlaps was the most time-consuming calculation, and to do it less frequently, this step was performed after step 3. 5) The cycle of steps 1–4 is repeated until the desired number of Monte Carlo trial moves has been executed. (Note that this sequence of events is different from in a more typical scenario when there are soft interactions. In the latter case, the acceptance criterion depends on the total energy of the system, which depends on the configuration of molecules; the move must then be attempted before the acceptance criterion is calculated and hence steps 3 and 4 must be reversed.) Because our solvent consists of a mixture of hard disks, we took advantage of scaled-particle theory to set the solvent activities, z_i, such that the equilibrium values of ρ_i^{bulk} were very close to the values we desired. As $\mu_i = kT\ln(\lambda_i^3\rho_i^{bulk}) + W_i$ (W_i is the work of inserting an i at a fixed site; see, e.g., (Ben-Naim, 1974), $z_i = \rho_i^{bulk}\exp(W_i/(kT))$. We obtained $W_i/(kT)$ from scaled-particle theory in two dimensions (Lebowitz et al., 1965). To increase the computational speed, we used the cell method of neighbor lists (see Allen and Tildesley, 1987) for the waters. For each binary solution (R_3/R_1, r_3^{bulk}, η), we performed at least six simulations with different random seeds to obtain statistics and error bars. Error bars were calculated as the standard error.

Calculation of Γ_3 and B^{fs}

During each simulation run, for each box (ms or bulk), we gathered $\langle N_1\rangle$ and $\langle N_3\rangle$ data. For the ms box, we also calculated $\rho_1(x)$ and $\rho_3(x)$, the average densities of water and cosolvent molecule centers, respectively, at a distance x from the hard wall. Fig. 3 *A*, shows an example of such a distribution.

We calculated Γ_3 based on its definition. If we divide Eq. 1 by the molecular weight of water, we see that Γ_3 can be recast in terms of the cosolvent(solute):water number ratios, r_i ($\equiv\langle N_i\rangle/\langle N_1\rangle$): $\Gamma_3 = \partial r_3/\partial r_2$. Because the ms box is essentially the bulk box with two solutes (two hard walls, far apart) added to it, we can directly calculate Γ_3 by approximating the derivative by a difference:

$$\Gamma_3 \sim \frac{\Delta r_3}{\Delta r_2}, \tag{6}$$

where Δ indicates the difference between the ms and bulk boxes (e.g., $\Delta r \equiv r^{ms} - r^{bulk}$). Let us now determine Δr_3 and Δr_2:

$$\Delta r_3 = \frac{\langle N_3^{ms}\rangle}{\langle N_1^{ms}\rangle} - \frac{\langle N_3^{bulk}\rangle}{\langle N_1^{bulk}\rangle} = \frac{\langle N_3^{bulk}\rangle + \langle \Delta N_3\rangle}{\langle N_1^{bulk}\rangle + \langle \Delta N_1\rangle} - \frac{\langle N_3^{bulk}\rangle}{\langle N_1^{bulk}\rangle} \tag{7}$$

and

$$\Delta r_2 = \frac{2}{\langle N_1^{ms}\rangle} - \frac{0}{\langle N_1^{bulk}\rangle} = \frac{2}{\langle N_1^{bulk}\rangle + \langle \Delta N_1\rangle}. \tag{8}$$

Because the ms box is dilute in solute, $\langle \Delta N_3\rangle \ll \langle N_3^{bulk}\rangle$ and $\langle \Delta N_1\rangle \ll \langle N_1^{bulk}\rangle$. Inserting Eqs. 7 and 8 into Eq. 6, and performing a Taylor's expansion keeping only first-order terms in $\langle \Delta N_3\rangle/\langle N_3^{bulk}\rangle$ and $\langle \Delta N_1\rangle/\langle N_1^{bulk}\rangle$, we obtain

$$2\Gamma_3 \sim \langle \Delta N_3\rangle - \frac{\langle N_3^{bulk}\rangle}{\langle N_1^{bulk}\rangle}\langle \Delta N_1\rangle = \langle \Delta N_3\rangle - r_3^{bulk}\langle \Delta N_1\rangle. \tag{9}$$

(The factor of 2 arises because there are two solutes.)

Note that this method of obtaining Γ_3 from a grand canonical simulation is different than that of Record and co-workers (Mills et al., 1986; Olmsted et al., 1989, 1991, 1995) who simulated without explicit water. Because our simulations contain explicit water, they are more useful for examining effects where the interactions with water are comparable in magnitude with interactions with cosolvent.

B_i^{fs} is defined as the number of i molecules within the first peak of $\rho_i(x)$:

$$B_i^{fs} = \int_0^{x_i^{min}} \rho_i(x')dx' \tag{10}$$

where x_i^{min} is the location of the first minimum in the $\rho_i(x)$ distribution (see, e.g., Fig. 3 *A*) and demarks the "end" of the first shell of species i; x_i^{min} is the thickness of a monolayer of i. Note that, as the cosolvent is larger than water, a cosolvent monolayer is thicker than a water monolayer ($x_3^{min} > x_1^{min}$).

In this paper, all lengths are reported in units of the water radius (i.e., a water radius is "1"). In the limit of dilute solute, the amount of solvent accumulated at a surface depends linearly on the surface area if the surface is uniform. Therefore, Γ_3, Γ_1, B_i, and B_i^{fs} are all proportional to the length of the hard wall. In this paper, Γ_3, Γ_1, B_i, and B_i^{fs} values are all reported per unit length ($=R_1$) of hard wall.

RESULTS

How B_i depends on the solvent near the solute

In practice, the local domain is demarked by the outer edge of a cosolvent monolayer; B_i depends mostly on B_i^{fs}.

First, we describe what a typical solvent distribution looks like. Fig. 3 *A* shows an example. There is an unambiguous, large first peak corresponding to the first layer of solvent and often several much smaller peaks corresponding to the second and further layers. These features of the distribution were observed for all the cosolvent sizes and solvent compositions, even those that were dilute in cosolvent. (These features are not artifacts of two dimensions because distributions of hard-sphere mixed solvents in three dimensions show the same behavior (Tan et al., 1989; Sokolowski and Fischer, 1990; Noworyta et al., 1998). The infinitely sharp first peak is due to the absence of soft interactions. For real solvents, the first peak would be softened with a leading edge of finite slope (compare Throop and Bearman (1965) with (1966)).)

If the solvent structure associated with the second and further shells is ignored, the approximated water and cosolvent $\rho(x)$ curves then look like Fig. 3 *B*. The local domain in this approximation has a well-defined outer boundary at the end of the cosolvent first shell (at x_3^{min}). Even though the water's properties are assumed to be bulk-like in the region beyond x_1^{min}, the overall binary solvent's properties are not bulk-like until x_3^{min}, and hence the region between x_1^{min} and x_3^{min} is still part of the local domain. The bulk domain is at $x > x_3^{min}$ in this approximation.

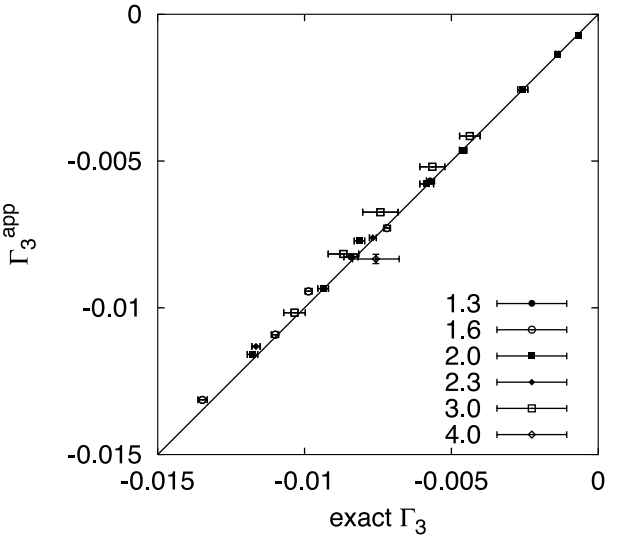

FIGURE 4 The bumps and wiggles in the solvent distribution associated with the second and further solvent layers can be ignored. If the peaks and valleys associated with these further solvent shells have been flattened to bulk density (see, e.g., Fig. 3 *B*), the resulting approximate preferential interaction coefficient (Γ_3^{app}) compares excellently to the exact Γ_3. The key indicates the values of R_3/R_1. Except where shown, the *y*-error bars are smaller than the points.

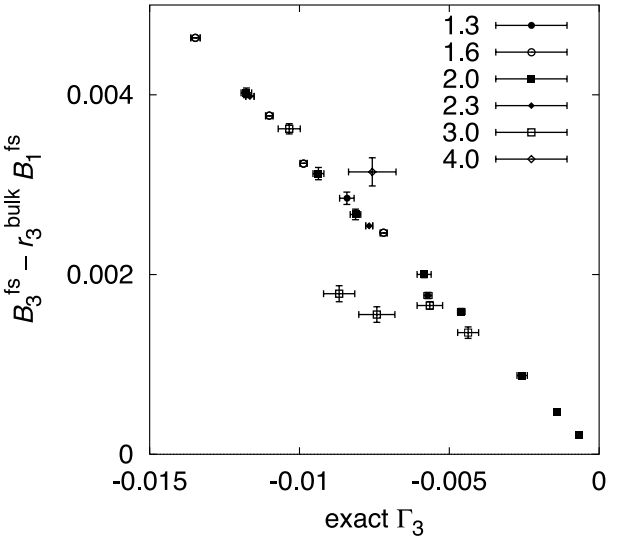

FIGURE 5 Assuming that B_1 is the amount of water in a water monolayer predicts the wrong sign for Γ_3. If it is assumed that B_i is the amount of *i* in an *i* monolayer, then $B_3^{fs} - r_3^{bulk}B_i^{fs}$ is the corresponding preferential interaction coefficient. Comparing these values with the exact Γ_3 values, we see that for all the mixed solvents we investigated, $B_3^{fs} - r_3^{bulk}B_1^{fs}$ values are positive, whereas the Γ_3 values are negative. (The key indicates the values of R_3/R_1; *y*-error bars for $R_3/R_1 = 1.6$ and 2.3 were omitted because they are smaller than the point.)

Let us now compare the preferential interaction coefficient associated with this approximate solvent distribution (we call it Γ_3^{app}) with the exact value. We calculate Γ_3^{app} using Eq. 2 with the B_i values corresponding to this approximate solvent distribution (B_i is obtained by integrating the approximate $\rho_i(x)$ out to x_3^{min}). B_1 and B_3 are represented by the vertically and horizontally hatched regions, respectively, in Fig. 3 *B*. Note that $B_1 \neq B_1^{fs}$ because more than first-shell waters are counted. Fig. 4 shows that Γ_3^{app} is an excellent approximation for Γ_3 for all solvent compositions and cosolvent sizes.

Also, to check the robustness of our results on overall solvent density, we increased the total packing fraction from 0.4 to 0.5 (which increases the solvent structure). For two solvent compositions with $R_3/R_1 = 2$, Γ_3^{app} still exactly agrees with Γ_3 (data not shown).

Γ_3 is indeed dominated by the first shells of water and cosolvent. The solvent structure associated with the second and higher shells can be mostly ignored for the purposes of determining Γ_3 and for understanding from where the dominant contributions to Γ_3 arise. Also, because the solvent beyond the first shells can be assumed to be bulk-like in density, the local domain in practice extends only to the end of the cosolvent monolayer.

A recipe for relating B_i to B_i^{fs} is given by Eqs. 4 and 5. ρ_1^{bulk} $(V_3^{fs} - V_1^{fs})$ counts the water molecules that would lie in the space between x_1^{min} and x_3^{min}. This region is part of the local domain and the waters in it must be counted in B_1. For our simple 2D model with a planar solute, $(V_3^{fs} - V_1^{fs}) = (x_3^{min} - x_1^{min}) \times$ [the length of the hard wall]. For a three-dimensional (3D) spherical solute of radius R_2, $(V_3^{fs} - V_1^{fs})$ would be $4/3\pi[(R_2 + x_3^{min})^3 - (R_2 + x_1^{min})^3]$.

Assuming that B_1 *counts only the water in a monolayer leads to the prediction of the wrong sign for* Γ_3

Various researchers (Zhang et al., 1996; Hammou et al., 1998; Courtenay et al., 2000a, b) have suggested obtaining B_1 from (or compared their predictions of B_1 to) the number of molecules within a monolayer of water, implying that $B_1 \sim B_1^{fs}$, omitting the waters in the volume $(V_3^{fs} - V_1^{fs})$. To find out whether this a good approximation, we set B_1 to B_1^{fs} and B_3 to B_3^{fs}, and calculated the corresponding preferential interaction coefficient, $B_3^{fs} - r_3^{bulk}B_1^{fs}$ (from Eq. 2). In Fig. 5, which compares the exact Γ_3 to $B_3^{fs} - r_3^{bulk}B_1^{fs}$, we see that this is clearly a bad approximation because $B_3^{fs} - r_3^{bulk}B_1^{fs} > 0$, whereas $\Gamma_3 < 0$. (When there are only excluded-volume interactions, the smaller species is always preferentially accumulated relative to the larger because the smaller molecules can better fit in the cavities and crevices between the larger ones and the solute surface. That's why potato chip crumbs are at the bottom of the bag.)

Assuming $B_1 \sim B_1^{fs}$ is a poor approximation because the number of waters counted in B_1 is too small. Because cosolvent molecules are almost always larger than water, the cosolvent monolayer is thicker than the water monolayer. The cosolvents counted in B_3 are in the shell $0 < x <$

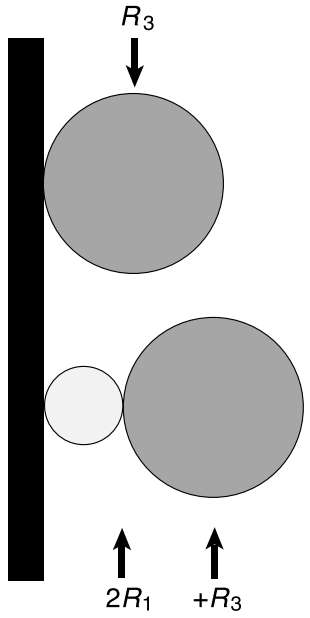

FIGURE 6 How thick is a cosolvent monolayer? This figure accompanies the heuristic argument in the text that describes where the peaks and valleys in the surface cosolvent distribution should be. It shows the molecular configurations corresponding to the first two peaks of the cosolvent distribution. The *dark gray circles* correspond to the cosolvent molecules for which $\rho_3(x)$ is observed; the *light gray circle* corresponds to the water that serves as a spacer between the wall and the observed cosolvent molecule.

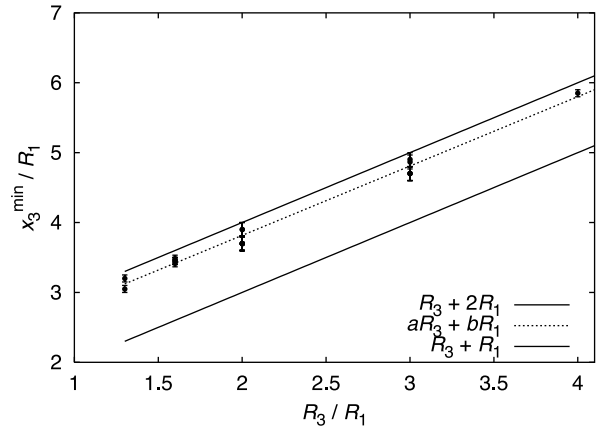

FIGURE 7 The thickness of a cosolvent monolayer increases linearly as a function of cosolvent size. The outer delimiter of the cosolvent monolayer, x_3^{min}, is shown as a function of cosolvent size (in units of R_1). For a given cosolvent, x_3^{min} depends only weakly on the solvent composition, so data for all solvent compositions are plotted together (x_3^{min} and x_1^{min} shift slightly closer to the solute surface as the cosolvent concentration increases; data not shown). The *heavy solid line* is our underestimate $x_3^{min} > R_3 + R_1$. $x_3^{min} \sim R_3 + 2R_1$ (*light solid line*) provides a rough rule of thumb for locating the end of the first cosolvent layer. The best-fit straight line, $x_3^{min} = aR_3 + bR_1$ where $a = 0.99 \pm 0.02$ and $b = 1.83 \pm 0.05$, is also shown (*dashed line*).

x_3^{min}, whereas the waters are counted from the thinner shell $0 < x < x_1^{min}$. The predicted Γ_3 is then too positive.

Even though we can ignore water's nonbulk properties beyond its first shell (and assume bulk behavior in these farther regions), we cannot ignore the actual water molecules beyond the water's first shell. Some of them still need to be counted in B_1. The region from which one counts water molecules to obtain B_1 must be the same as that from which one counts cosolvent molecules for B_3 (more below).

How thick is a cosolvent monolayer?

We've established earlier that, for practical purposes, the local domain extends only to the end of the cosolvent first shell. How far from the surface is that?

Let us describe in physical terms approximately where the peaks and troughs in the $\rho_3(x)$ distribution should lie. (The argument is based on that by Ben-Naim (1974) to understand the radial distribution functions ($g(r)$) of a binary solution.) Fig. 6 shows the configurations corresponding to the first two peaks of the cosolvent distribution. The *dark gray* molecules are the cosolvent molecules under "observation," i.e., the ones for which $\rho_3(x)$ is considered. The *light gray* molecule, which is usually a water because most molecules are waters, fills the space between the observed cosolvent and the wall. We see that in the cosolvent distribution, the first and second peaks lie approximately distances R_3 (plus a little for thermal motion) and $2R_1 + R_3$ (plus a little) from the wall, respectively. The first minimum (the end of the first cosolvent peak) should lie somewhere in between, $\sim R_1 + R_3$ (plus some) from the wall.

To demonstrate that this rough argument holds, at least for our simple solvent system, in Fig. 7 we graph x_3^{min} as a function of cosolvent size. The *heavy solid line* is our heuristic lower bound for the location of the x_3^{min}. We find that as a rough rule of thumb that $x_3^{min} \sim 2R_1 + R_3$, which is shown as the *light solid line*. In other words (plus some) is about a water's radius.

Because this heuristic argument only assumes that hard interactions are the primary determinants of the packing arrangement of a liquid (it has been argued that this is true for many liquids (Reiss, 1966)), it should roughly hold for real solvents against a real solute surface. If, however, other interactions predominate the packing arrangment, this argument should break down.

Because the local domain's size grows with the cosolvent, for larger cosolvents, one must count more water layers to determine B_1 than for smaller ones. The local domains of even moderately sized cosolvents can extend quite a bit beyond a water monolayer. For example, when $R_3/R_1 = 3.0$ (corresponding in size to sucrose), the local domain and B_i encompass two water layers (data not shown).

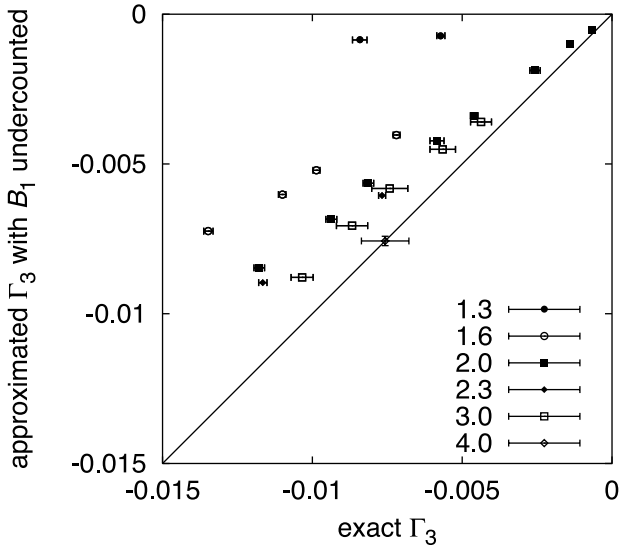

FIGURE 8 The region from which one counts water molecules for B_1 must be the same as that from which one counts cosolvent molecules for B_3. This figure is the same as Fig. 4 except that instead of counting waters to the end of the cosolvent first shell (to $x^{min}{}_3$), we stopped $0.2R_1$ shy of it (to $x^{min}{}_3$ $0.2R_1$). The key indicates the values of R_3/R_1 and the y-error bars were smaller than the points, except where shown. With B_1 just slightly undercounted, the predicted Γ_3 values are quantitatively off.

When determining B_1*, count waters from the same region of space as when determining* B_3

We wish to emphasize, at this point, that when counting water molecules for B_1, one needs to count molecules from the same region of space as when counting cosolvent molecules. Above, we showed that when B_1 counts waters to the end of the water first shell (to $x_1^{\min}$) and B_3 counts cosolvent molecules to the end of the cosolvent first shell (to $x_3^{\min}$), the predicted Γ_3 values had the wrong sign.

Next, we show that even if there is a small difference in the regions from which one counts water and cosolvent molecules, the resulting error in Γ_3 is not small. Say the region from which one counts the water molecules is just $0.2R_1$ too narrow. For $R_3/R_1 = 1.3$, the region from which one counts water molecules is then 7% smaller than that from which one counts cosolvent molecules; for $R_3/R_1 = 3.0$, the difference in the sizes of the regions is 4%. (Note, not all of this region is occupied, the slice at $x < R_1$ being free of solvent centers. If we consider only the regions occupied by solvent centers, then the size differences are 10% and 6% for $R_3/R_1 = 1.3$ and 3.0, respectively.) The predicted Γ_3 values (shown in Fig. 8) not surprisingly are less negative than the exact values because the B_1 values are too small. The deviation from the correct Γ_3 values is quite large—tens of percentage points. Our results are for a planar macromolecular surface. If the macromolecule is spherical, then the error in Γ_3 would be larger due to the x^2 dependence of the volume of thin spherical shells.

The reason Γ_3 is sensitive to errors in B_i is because it is the small difference of two larger numbers, and any error in one of the larger numbers causes a significant error in Γ_3. To see this one can think of B_i as the amount of solvent that would be in the local domain if there were no solute, B_i^{bulk}, plus the solute-induced deviation ∂B_i; $B_i = B_i^{bulk} + \partial B_i$. When the regions for counting waters for B_1 and cosolvent molecules for B_3 are the same, the B_3^{bulk} and B_i^{bulk} terms exactly cancel and $\Gamma_3 = \partial B_3 - (m_3^{bulk}/m_1)\partial B_1$. The difference between two large numbers comes from this exact cancellation. If one erroneously counts waters from a different region than that from which the cosolvent molecules are counted, the B_3^{bulk} and B_1^{bulk} terms do not cancel, and this is where the error lies.

For real solvents and solutes, these results may serve as a first-order approximation for the major contributors to Γ_3

Because we studied a simple solvent-solute system, it is not a priori clear how our results apply to real solvents and solutes. Below, we present two pieces of indirect evidence that our system bears resemblance to real solvents and we discuss the physical arguments that suggest that for some cosolvents our results may serve as a first-order approximation for the major contributors to Γ_3.

First, experimental data show that Γ_3 is proportional to m_3^{bulk} over a wide range of cosolvent concentrations (Courtenay et al., 2000a). Despite the differences in physical model, our simulations show similar results. Over the range of cosolvent concentrations we used, plots of Γ_3 versus r_3^{bulk} are mainly linear for low-to-moderate cosolvent concentrations with slight upward curvature at higher r_3^{bulk} (data not shown). With $R_3/R_1 = 3$, when $r_3^{bulk} \leq 0.036$ (corresponding to the cosolvent:water total "volume" ratio $\leq$0.32, which is distinctly above the dilute cosolvent limit), a straight-line fit gives $\Gamma_3 = -0.168\ (\pm 0.005) \times r_3^{bulk}$ with reduced $\chi^2 = 0.70$. With $R_3/R_1 = 2$, when $r_3^{bulk} \leq 0.031$ (corresponding to the cosolvent:water total "volume" ratio $\leq$0.12), a similar fit yields $\Gamma_3 = -0.089\ (\pm 0.002) \times r_3^{bulk}$ with reduced $\chi^2 = 0.57$.

Second, we calculated the local-bulk partition coefficient, K_p, to see whether the simple hard interactions of our model can induce as much nonbulk character at a solute surface as is seen for real solvents. K_p compares the local cosolvent:water ratio to that of bulk (Courtenay et al., 2000a):

$$K_p \equiv \frac{\text{cosolvent:water mole ratio in the local domain}}{\text{cosolvent:water mole ratio in the bulk domain}} = \frac{B_3/B_1}{m_3^{bulk}/m_1}. \quad (11)$$

We demonstrate below that K_p values obtained from our model are of the same magnitude as experimental values.

Courtenay et al. (2000a) showed that, if it is assumed that the amount of water in the local domain is the same as when the solute is immersed in pure water (which is probably the case when the solvent is infinitely dilute in cosolvent), K_p can be related to Γ_3 by

$$\frac{\Gamma_3/\mathrm{ASA}}{m_3^{\mathrm{bulk}}} = \frac{(K_p - 1)b_1^{\circ}}{m_1} \tag{12}$$

where Γ_3/ASA is the preferential interaction coefficient per water-accessible surface area, and $b_1°$ is the amount of water, per accessible surface area, in the local domain when the solute is immersed in pure water. We calculated K_p values for our simple system using Eq. 12 with the left-hand side obtained from the slope of Γ_3 as a function of r_3^{bulk} in the linear regime (see previous paragraph), and $b_1°$ values obtained from simulations with pure water. For $R_3/R_1 = 2$, $K_p = 0.67$; for $R_3/R_1 = 3$, $K_p = 0.39$. We compare our K_p values with experimental values for "neutral" cosolvents (urea, glycerol, trehalose, trimethylamine N-oxide, proline, and betaine glycine); the latter vary between 0.14 (betaine glycine) to 1.12 (urea) (Courtenay et al., 2000a). We see that the K_p values obtained on our simple solvent system are of the same order of magnitude as those from experiment for neutral cosolvents. This suggests that the forces within our simple system (which cause the solvent composition in the local domain to deviate from that of bulk) may be of similar magnitude to the forces between real solvents and solutes. Hence, the results from our simple model may have some bearing on real systems. The similarity of the magnitudes of the simple-model and experimental K_p values also suggests that excluded-volume forces may play a large role in the depletion of neutral cosolvents near real solute surfaces. (Now, we comment further on the calculation of K_p. Because the experimental K_p values of Courtenay et al. use the amount of water within a water monolayer for $b_1°$ (Courtenay et al., 2000a), we have done the same solely for the purpose of comparing our K_p values to those of Courtenay et al. Except when the cosolvent is completely excluded, including only a water monolayer in $b_1°$ provides only an imprecise lower bound on the degree of hydration (Courtenay et al., 2000a). The resulting values of $K_p - 1$ may be too large, and the correct K_p values may be closer to 1 (implying less disturbance of the local solvent compared to bulk).)

Earlier, we showed that, for our simple model, the local domain is demarked by the outer edge of a cosolvent monolayer. A recipe for relating B_i to B_i^{fs} is given by Eqs. 4 and 5. Does this conclusion apply to real solvents and solutes? The main assumption here was that the amount of solvent structure beyond the first shell is negligible compared to that of the first shell. More explicitly, the heights of the second and further peaks in the surface solvent distribution are much smaller than that of the first peak (corresponding to the monolayer), and that the deviation from the bulk composition in these more distant regions plays a negligible role compared to the region near the solute. To determine the applicability of this assumption and the resulting conclusions to real solvents and solutes, we examined the surface solvent distributions obtained from experiments on and atomic-resolution computer simulations of proteins and DNA in pure water and in neutral mixed solvents. Because there were usually only one or two peaks visible in $\rho_i(x)$ (see, e.g., Burling et al., 1996; Tirado-Rives et al., 1997; Sprous et al., 1998; Pettitt et al., 1998), long-ranged solvent structure appears to be absent in these systems. Hence, we believe that for at least these real mixed solvent/solute systems with mainly short-ranged solvent structure, the results determined from our study will serve as a first-order approximation for Γ_3 (and may possibly do better) and that the recipe given by Eqs. 4 and 5 should provide the largest contribution to Γ_3. (The lack of extensive structure for real solvents near real solutes may be due to the larger number of length scales than in our simple system and to the bumpiness of the macromolecular surface.) If, however, the solvent displays significant long-ranged structure (i.e., if the degree of structure associated with the second and higher shells is significant compared to that of the first), or if either solvent species is strongly excluded from the solute surface (leading to a depletion of that species in the first shell), our results probably would not apply because the fundamental assumptions are likely not true. (For example, the surface distribution of charged species can have more than one large peak or can be quite long-ranged. See, e.g., the distribution of cations and anions at the surface of a methane solute (Smith, 1999) and the radial distribution functions of mixed solvents (Chitra and Smith, 2000).)

Additionally, we concluded that when determining B_1, it is important to count waters from the same region of space as when counting cosolvent molecules for determining B_3; assuming that B_1 counts only a water monolayer results in a poor approximation for Γ_3, at least in our 2D, hard disk model system. This view of the local domain and the main contribution to Γ_3 is different from that of Courtenay et al. (2000a, b), who analyzed Γ_3 data for the highly excluded betaine glycine and found that if they assumed complete exclusion ($K_p = 0$ and $B_3 = 0$), this would predict $b°_1$ to be close to a water monolayer. This led to their "working hypothesis" that the amount of water in the local domain (estimated with an excluded solute) is a monolayer. Accumulation of a cosolvent molecule at the solute surface ($K_p > 0$; $B_3 > 0$) is modeled as replacement of water by cosolvent, based on relative molecular cross-sectional areas. This interpretation of the local-bulk domain model by Courtenay et al. is consistent with the extant data on Γ_3 for solute-biopolymer interactions and solute effects on biopolymer

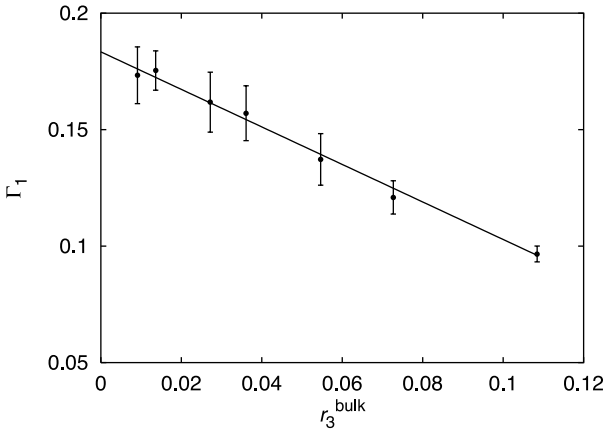

FIGURE 9 Even in the absence of specific interactions, Γ_1 still depends on the cosolvent concentration. Shown are data for a cosolvent with $R_3/R_1 = 3.0$. The straight line is the best linear fit with the intercept equal to 0.183 ± 0.002 and a slope of -0.81 ± 0.02.

processes (Courtenay et al., 2000a, b). Despite the differences in physical model, our values of Γ_3 and K_p behave similarly to those of real mixed solvents (see above). Without simulations of the hard sphere model in three dimensions with which one could make direct comparisons with experiment, it is not clear how to distinguish between these two pictures.

All of these results apply to Γ_3 data obtained under dialysis conditions. We do not know whether they apply to other thermodynamic ensembles. The two-domain model was derived for preferential interaction coefficients measured under dialysis conditions (Record and Anderson, 1995), and to our knowledge, it has not been extended to other ensembles. In addition, although Schellman (1990) has suggested that preferential interaction coefficients measured under isopiestic, dialysis, and electrochemical cell (constant cosolvent chemical potential) conditions should not differ much, in practice this is not the case for some cosolvents (see Courtenay et al., 2000a).

Test of a steric-exclusion model of preferential hydration

Timasheff and co-workers put forth a steric-exclusion model for preferential hydration (Arakawa and Timasheff, 1985; Bhat and Timasheff, 1992) founded on an idea proposed by Kauzmann, as cited by Schachman and Lauffer (1949). In this model, the cosolvent molecules are limited in their approach to the solute. There is an exclusion shell of thickness R_3 which contains no cosolvent molecule centers, and it is thought that, when the binary solution is dilute in cosolvent, the exclusion shell is filled with pure bulk water. (Note that there may be parts of cosolvent molecules in the exclusion shell, even if the cosolvent center cannot lie within it.) Outside the exclusion shell, the distributions of water and cosolvent are assumed to be those of the bulk mixed solvent. The excess water and lack of cosolvent in the exclusion shell lead to preferential hydration ($\Gamma_1^{(e)} > 0$; the superscript indicates the limit of dilute cosolvent).

The solvent distribution as approximated by this model does not reflect the true solvent distribution. Certainly $\rho_3(x)$ is 0 within the exclusion shell $0 < x < R_3$. However, $\rho_3(x)$ is not featureless, like that of bulk solvent, outside the exclusion shell. We find in our simulations of various solvent compositions with $R_3/R_1 = 2.0$ and 3.0 that all surface cosolvent distributions have a dominant first peak starting at $x = R_3$, even when the cosolvent concentration is low. The height of this peak—the density of cosolvent right up against the surface—is several times that of the bulk density; this observation is independent of the cosolvent concentration. In other words, the "structure" in the cosolvent distribution doesn't diminish as the cosolvent concentration is lowered. Likewise, the solvent distribution of the water is not steplike, as assumed in the steric-exclusion model, but has the usual dominant first peak plus smaller wiggles further out. Also, data from small-angle x-ray and neutron scattering indicate that the water at a protein surface is 10% denser than in neat water (Svergun et al., 1998). The solvent distribution assumed by the steric-exclusion model does not well reflect the true solvent distribution, at least not for these smaller cosolvents with $R_3/R_1 = 2.0$ and 3.0. (However, it is possible that the steric-exclusion shell of very large cosolvents is so thick, encompassing many water layers, that on average the water distribution within the shell may be like that of neat water. The steric-exclusion model's picture of the water distribution may be more accurate for these very large cosolvents. Unfortunately, our Monte Carlo algorithm is not able to sample such large cosolvents at dilute cosolvent concentration, and we know of no such simulations done by other researchers.)

We also believe that the assumptions on the solvent distribution in the steric-exclusion model are not accurate for the purposes of determining $\Gamma_1^{(e)}$. In the model, any solvent structure beyond the sterically excluded shell is assumed to be negligible. The local domain then comprises only the steric-exclusion shell, $x < R_3$. Within this shell there are no cosolvent molecule centers, so B_3 is set to zero. In other words, this model assumes the $(m_1/m_3^{bulk})B_3$ term in Eq. 3 to be negligible compared to the B_1 term. However, since $m_1/m_3^{bulk} = 1/r_3^{bulk} \rightarrow \infty$, dividing by r_3^{bulk} brings any bumps and wiggles in the cosolvent distribution to a size comparable to those in the water distribution. One expects, then, the $(m_1/m_3^{bulk})B_3 = B_3/r_3^{bulk}$ term should be roughly the same order of magnitude as the B_1 term, and thus cannot be ignored. Indeed, for the most dilute solutions for which we obtained $\rho(x)$ data ($R_3/R_1 = 3.0$, $r_3^{bulk} = 0.027$ and $R_3/R_1 = 2.0$, $r_3^{bulk} = 0.0077$), this is the case. In addition, for all the

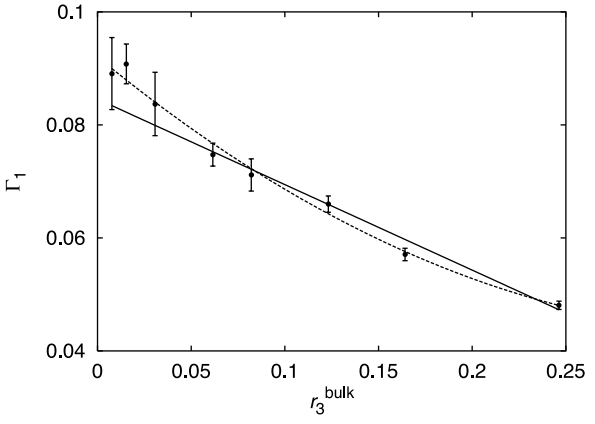

FIGURE 10 Same as Fig. 9 except with $R_3/R_1 = 2.0$. The *solid line* is the best-fit straight line with intercept 0.085 ± 0.002 and slope of -0.15 ± 0.01. The best-fit second-order polynomial, $ar^2 + br + c$ where $r = r_3^{bulk}$ and $a = 0.38 \pm 0.10$, $b = -0.27 \pm 0.03$ and $c = 0.092 \pm 0.002$, is also shown (*dashed line*).

solvents we studied, the first layer of cosolvent contributes as much to $\Gamma_1^{(e)}$ as the water within the exclusion shell.

Next, we tested the prediction of $\Gamma_1^{(e)}$ based on the steric-exclusion model against the $\Gamma_1^{(e)}$ values from our simulation (obtained by extrapolating Γ_1 to $r_3^{bulk} \rightarrow 0$). For $R_3/R_1 = 3.0$ (Fig. 9), a straight-line fit yields $\Gamma_1^{(e)} = 0.183 \pm 0.002$. Now, what does the steric-exclusion model predict for $\Gamma_1^{(e)}$? In this model B_3 is set to zero and B_1 is the amount of neat water that fits in a shell of thickness R_3 at the solute surface. Carrying over the steric-exclusion model to two dimensions with a planar solute, the model predicts that the preferential hydration per unit length of wall is $\Gamma_1^{(e)} = n_1^\circ R_3 R_1$, where n_1° is the number density of neat water; $n^\circ{}_1^\circ = \eta/(\pi R_1{}^2)$. (The factor of R_1 in the formula for $\Gamma_1^{(e)}$ arises because the unit length is equal to R_1.) Assuming that the packing fraction of neat water remains $\eta = 0.4$, then the model predicts that $\Gamma_1^{(e)} = 0.38$, in poor agreement with the actual $\Gamma_1^{(e)}$ value. Now, let us perform the same analysis for $R_3/R_1 = 2.0$ (see Fig. 10). The value of $\Gamma_1^{(e)}$ is 0.085 ± 0.002 (0.092 ± 0.002) for a linear (quadratic) fit of the Γ_1 versus r_3^{bulk} data. The steric-exclusion model predicts $\Gamma_1^{(e)} = 0.25$, which again doesn't agree. In summary, the steric-exclusion model makes poor approximations of $\Gamma_1^{(e)}$ for both cosolvents ($R_3/R_1 = 2$ and 3).

We also point out that the preferential hydration values do depend on the cosolvent concentration, even though specific interactions are absent and all solvent species are chemically inert. Γ_1 decreases as the concentration of cosolvent increases (see Figs. 9 and 10). For $R_3/R_1 = 3$, Γ_1 drops by a factor of about two as the total cosolvent:water volume ratio rises from near zero to 0.98. Similar behavior has been observed for polyethylene glycols at protein surfaces (Arakawa and Timasheff, 1985; Bhat and Timasheff, 1992). This anticorrelation of Γ_1 with cosolvent concentration must at least be partly due to excluded-volume interactions, because those are the only interactions present in our simulations.

CONCLUSIONS

When the preferential interaction coefficient, Γ_3, is measured in a dialysis equilibrium experiment, it can be related to the solvent distribution surrounding the solute by Eq. 2, where B_1 and B_3 are the numbers of water and cosolvent molecules, respectively, in the local domain, the region of solvent that displays nonbulk characteristics (Record and Anderson, 1995). This relationship (for uncharged solute and solvent) is exact, but in practice it is not so useful for understanding solute-solvent interactions because the local domain has an ill-defined boundary and it is unclear which solvent molecules are counted in B_i, and are thereby sampled by Γ_3. Also, the local domain can extend quite far from the solute, tens of nanometers in some cases (see Blokzijl and Engberts, 1993; Vogler, 1998, and references therein), and solvent molecules distant from the solute may contribute to B_1 and B_3, and therefore to Γ_3. However, because most of the nonbulk structure is associated with the solvent right next to the solute, one expects that Γ_3 should mostly depend on the nearby solvent, and not on farther reaches of the local domain, and therefore the B_i values should mostly count the solvent close to the solute. We find that this is indeed true. In practice, the outer boundary of the local domain is demarked by a cosolvent (not water) monolayer if solvent structure is short-ranged. Also, the second and further solvent shells can mostly be ignored (again, if solvent structure is short-ranged). A recipe for approximating the B_i values is given by Eqs. 4 and 5: B_3 can be set to the amount of cosolvent in a monolayer; B_1 is the amount of water in a monolayer plus the amount of water that would lie between the end of the water first shell and the end of the cosolvent first shell, if that space were filled with bulk mixed solvent.

Positioning the local domain's boundary at the outer edge of the cosolvent monolayer is a practical, not exact, definition for the purpose of interpreting Γ_3 data. The basic physical principle underlying this result is that the amount of solute-induced solvent structure associated with the second and further solvent shells is small compared to that of the first shell, and hence these further shells, to a first-approximation, can be ignored. This result, of course, applies directly only to our simple 2D, hard-disk solvent model and the conditions under which we performed our simulation. Also, for solvents with long-ranged solvent structure (i.e., with a second solvent shell of significant size compared to the first shell) or for those that are strongly repelled from the solute (in which case the first shell is diminished or absent), this rule of thumb would not be

expected to apply. However, because the solvent distributions of water and some neutral mixed solvents at the surfaces of proteins and DNA (as obtained by experiments and atomic-resolution simulations) show neither significant long-ranged solvent structure nor strong solvent repulsion (see Burling et al., 1996; Tirado-Rives et al., 1997; Sprous et al., 1998; Pettitt et al., 1998), locating the local domain's boundary at the outer edge of the first cosolvent shell might serve as a first-order approximation for the dominant contribution to Γ_3 for some real cosolvents and solutes as well.

When determining B_1 and B_3, it is important to count water and cosolvent molecules from within the same region of space. If one counts water molecules from a region that is slightly different from that from which one counts cosolvent molecules, the resulting error in Γ_3 is not small, Γ_3 being sensitive to differences in the regions. If, for example, one were to assume that B_1 is the number of waters within a monolayer of water (i.e., assuming $B_1 \sim B_1^{fs}$, omitting the waters that lie between the end of the water first shell and the end of the cosolvent first shell) and that B_3 is the number of cosolvent molecules within a monolayer of cosolvent (i.e., $B_3 \sim B_3^{fs}$), then one would predict the wrong sign for Γ_3 (Fig. 5). Even small discrepancies between the two regions leads to a larger error in Γ_3 (Fig. 8).

Because as a first approximation the outer edge of the cosolvent first shell demarks (in practice if not in principle) the outer limit of the local domain, one would like to know approximately where that location is. We have presented a heuristic argument to show that the end of the cosolvent first shell should lie a distance $R_3 + R_1$ (plus some) from the solute surface. For our system of hard-disks up against a flat hard wall, (plus some) is about R_1 (see Fig. 7). For real solvents by a real solute surface, if solvent structure is short-ranged, we expect (plus some) to be of similar magnitude.

One of the implications of our findings is that the local domain is not a fixed region of space around the solute. It depends on the cosolvent size, larger cosolvents giving rise to larger local domains, which means more water layers to include in B_1. (Even for $R_3/R_1 = 3.0$, corresponding to the sucrose:water radius ratio, around two layers of water are included in B_1.) This makes comparison of preferential interaction data for differently sized cosolvents somewhat complicated, because the Γ_3 data count solvent from different regions of space. Also, because more than one water layer is often included in B_1, interpreting B_1 as the amount of contacting water or the amount of water in a monolayer is not accurate.

Because our model of the solvent and solute has only excluded-volume interactions, our results demonstrate what may happen when interactions are "neutral." For every solvent composition and cosolvent size we investigated in our model system, the surface cosolvent distribution is not in any way featureless. The first layer of cosolvent at the solute surface always has a density several times that of the bulk solvent. Therefore, even when interactions are fairly "neutral," one cannot ignore the cosolvent and view things only from the point of view of the water (or vice versa). B_1 and B_3 are not zero. Lastly, we tested a steric-exclusion model of preferential hydration. Assumptions about the solvent distribution are nonphysical, and the model made poor predictions of Γ_1.

We are grateful to Tack Kuntz for the potato chip-crumb analogy, to Johan van der Maarel and Kevin Silverstein for encouragement, to Tom Record for suggesting the calculation of K_p, and to the reviewers for helpful suggestions and comments. We thank the University of Minnesota's College of Biological Sciences' Advanced Biosciences Computing Center and the University of Minnesota Supercomputing Institute for computational resources.

This work was supported in part by National Institutes of Health Grant GM28093.

REFERENCES

Allen, M. P., and D. J. Tildesley. 1987. Computer Simulation of Liquids. Clarendon Press, Oxford.

Arakawa, T., and S. N. Timasheff. 1982a. Preferential interactions of proteins with salts in concentrated solutions. *Biochemistry.* 21: 6545–6552.

Arakawa, T., and S. N. Timasheff. 1982b. Stabilization of protein structure by sugars. *Biochemistry.* 21:6536–6544.

Arakawa, T., and S. N. Timasheff. 1985. Mechanism of poly(ethylene glycol) interaction with proteins. *Biochemistry.* 24:6756–6762.

Beglov, D., and B. Roux. 1996. Solvation of complex molecules in a polar liquid: an integral equation theory. *J. Chem. Phys.* 104:8678–8689.

Ben-Amotz, D., and K. G. Willis. 1993. Molecular hard-sphere volume increments. *J. Phys. Chem.* 97:7736–7742.

Ben-Naim, A. 1974. Water and Aqueous Solutions. Plenum Press, New York.

Bhat, R., and S. N. Timasheff. 1992. Steric exclusion is the principal source of the preferential hydration of proteins in the presence of polyethylene glycols. *Protein Sci.* 1:1133–1143.

Blokzijl, W., and J. B. F. N. Engberts. 1993. Hydrophobic effects. Opinions and facts. *Angew. Chem. Int. Ed. Engl.* 32:1545–1579.

Bull, H. B., and K. Breese. 1968. Protein hydration. I. Binding sites. *Arch. Biochem. Biophys.* 128:488–496.

Burling, F. T., W. I. Weis, K. M. Flaherty, and A. T. Brunger. 1996. Direct observation of protein solvation and discrete disorder with experimental crystallographic phases. *Science.* 271:72–77.

Casassa, E. F., and H. Eisenberg. 1964. Thermodynamic analysis of multicomponent solutions. *Advan. Protein. Chem.* 19:287–395.

Chitra, R., and P. E. Smith. 2000. Molecular dynamics simulations of the properties of cosolvent solutions. *J. Phys. Chem. B.* 104:5854–5864.

Courtenay, E. S., M. W. Capp, C. F. Anderson, and M. T. Record, Jr. 2000a. Vapor pressure osmometry studies of osmolyte-protein interactions: implications for the actions of osmoprotectants in vivo and for the interpretation of "osmotic stress" experiments in vitro. *Biochemistry.* 39:4455–4471.

Courtenay, E. S., M. W. Capp, R. M. Saecker, and M. T. Record, Jr. 2000b. Thermodynamic analysis of interactions between denaturants and protein surface exposed on unfolding: interpretation of urea and guanidinium chloride *m*-values and their correlation with changes in accessible surface area (ASA) using preferential interaction coefficients and the local-bulk domain model. *Proteins: Struct., Funct., Genet.* (Suppl 4): 72–85.

Edward, J. T. 1970. Molecular volumes and the Stokes-Einstein equation. *J. Chem. Ed.* 47:261–270.

Eisenberg, H. 1976. Biological Macromolecules and Polyelectrolytes in Solution. Clarendon Press, Oxford.

Eisenberg, H. 1994. Protein and nucleic acid hydration and cosolvent interactions: establishment of reliable baseline values at high cosolvent concentrations. *Biophys. Chem.* 53:57–68.

Gerstein, M., and R. M. Lynden-Bell. 1993. Simulation of water around a model protein helix. 1. Two-dimensional projections of solvent structure. *J. Phys. Chem.* 97:2898–2990.

Hammou, H. O., I. M. Plaza del Pino, and J. M. Sanchez-Ruiz. 1998. Hydration changes upon protein unfolding: cosolvent effect analysis. *New J. Chem.* 22:1453–1461.

Inoue, H., and S. N. Timasheff. 1972. Preferential and absolute interactions of solvent component with proteins in mixed solvent system. *Biopolymers.* 11:737–743.

Komeiji, Y., M. Uebayasi, J. Someya, and I. Yamato. 1993. A molecular dynamics study of solvent behavior around a protein. *Proteins: Struct., Funct., Genet.* 16:268–277.

Kuntz, I. D. 1971. Hydration of macromolecules. III. Hydration of polypeptides. *J. Am. Chem. Soc.* 93:514–516.

Kuntz, Jr., I. D., and W. Kauzmann. 1974. Hydration of proteins and polypeptides. *Adv. Protein Chem.* 28:239–345.

Lebowitz, J. L., E. Helfand, and E. Praestgaard. 1965. Scaled particle theory of fluid mixtures. *J. Chem. Phys.* 43:774–779.

Lee, J. C., and L. L. Y. Lee. 1979. Interaction of calf brain tubulin with poly(ethylene glycols). *Biochemistry.* 18:5518–5526.

Lee, J. C., and L. L. Y. Lee. 1981. Preferential solvent interactions between proteins and polyethylene glycols. *J. Biol. Chem.* 256:625–631.

Lee, J. C., and S. N. Timasheff. 1974. Partial specific volumes and interactions with solvent components of proteins in guanidine hydrochloride. *Biochemistry.* 13:257–265.

Lee, J. C., and S. N. Timasheff. 1981. The stabilization of proteins by sucrose. *J. Biol. Chem.* 256:7193–7201.

Levitt, M., and B. H. Park. 1993. Water: now you see it, now you don't. *Structure.* 1:223–226.

Liepinsh, E., and G. Otting. 1997. Organic solvents identify specific ligand binding sites on protein surfaces. *Nat. Biotech.* 15:264–268.

Liepinsh, E., P. Sodano, S. Tassin, D. Marion, F. Vovelle, and G. Otting. 1999. Solvation study of the non-specific lipid transfer protein from wheat by intermolecular NOEs with water and small organic molecules. *J. Biomol. NMR.* 15:213–225.

Lounnas, V., B. M. Pettitt, and G. N. Phillips. 1994. A global model of the protein-solvent interface. *Biophys. J.* 66:601–614.

Makarov, V. A., B. K. Andrews, and B. M. Pettitt. 1998. Reconstructing protein-water interface. *Biopolymers.* 45:469–478.

Mills, P., C. F. Anderson, and M. T. Record, Jr. 1986. Grand canonical Monte Carlo calculations of thermodynamic coefficients for a primitive model of DNA-salt solutions. *J. Phys. Chem.* 90:6541–6548.

Na, G. C., and S. N. Timasheff. 1981. Interaction of calf brain tubulin with glycerol. *J. Mol. Biol.* 151:165–178.

Noworyta, J., D. Henderson, S. Sokolowski, and K.-Y. Chan. 1998. Hard sphere mixtures near a hard wall. *Mol. Phys.* 95:415–424.

Olmsted, M. C., C. F. Anderson, and M. T. Record, Jr. 1989. Monte Carlo description of oligoelectrolyte properties of DNA oligomers: range of the end effect and the approach of molecular and thermodynamic properties to the polyelectrolyte limits. *Proc. Natl. Acad. Sci. U.S.A.* 86: 7766–7770.

Olmsted, M. C., C. F. Anderson, and M. T. Record, Jr. 1991. Importance of oligoelectrolyte end effects for the thermodynamics of conformational transitions of nucleic acid oligomers: a grand canonical Monte Carlo analysis. *Biopolymers.* 31:1593–1604.

Olmsted, M. C., J. P. Bond, C. F. Anderson, and M. T. Record, Jr. 1995. Grand canonical Monte Carlo molecular and thermodynamic predictions of ion effects of binding of an oligocation (L^{8+}) to the center of DNA oligomers. *Biophys. J.* 68:634–647.

Otting, G. 1997. NMR studies of water bound to biological molecules. *Prog. NMR spectrosc.* 88:1308–1314.

Otting, G., E. Liepinsh, and K. Wüthrich. 1991. Protein hydration in aqueous solution. *Science.* 254:974–980.

Parsegian, V. A., R. P. Rand, and D. C. Rau. 1995. Macromolecules and water: probing with osmotic stress. *Methods Enzymol.* 259:43–94.

Parsegian, V. A., R. P. Rand, and D. C. Rau. 2000. Osmotic stress, crowding, preferential hydration, and binding: a comparison of perspectives. *Proc. Natl. Acad. Sci. U.S.A.* 97:3987–3992.

Pessen, H., and T. F. Kumosinsky. 1985. Measurements of protein hydration by various techniques. *Methods Enzymol.* 117:219–255.

Pettitt, B. M., V. A. Makarov, and B. K. Andrews. 1998. Protein hydration density: theory, simulations and crystallography. *Curr. Opin. Struct. Biol.* 8:218–221.

Ponstingl, H., and G. Otting. 1997. Detection of protein-ligand NOEs with small, weakly binding ligands by combined relaxation and diffusion filtering. *J. Biomol. NMR.* 9:441–444.

Record, Jr., M. T., and C. F. Anderson. 1995. Interpretation of preferential interaction coefficients of nonelectrolytes and of electrolyte ions in terms of a two-domain model. *Biophys. J.* 68:786–794.

Record, Jr., M. T., W. Zhang, and C. F. Anderson. 1998. Analysis of effects of salts and uncharged solutes on protein and nucleic acid equilibria: a practical guide to recognizing and interpreting polyelectrolyte effects, Hofmeister effects, and osmotic effects of salts. *Adv. Protein. Chem.* 51:281–353.

Reisler, E., Y. Haik, and H. Eisenberg. 1977. Bovine serum albumin in aqueous guanidine hydrochloride solutions. Preferential and absolute interactions and comparison with other systems. *Biochemistry.* 16: 197–202.

Reiss, H. 1966. Scaled particle methods in the statistical thermodynamics of fluids. *Adv. Chem. Phys.* 9:1–84.

Rupley, J. A., and G. Careri. 1991. Protein hydration and function. *Adv. Protein Chem.* 41:37–172.

Schachman, H. K., and M. A. Lauffer. 1949. The hydration, size and shape of tobacco mosaic virus. *J. Am. Chem. Soc.* 71:536–541.

Schellman, J. A. 1990. A simple model for solvation in mixed solvents. Applications to the stabilization and destabilization of macromolecular structures. *Biophys. Chem.* 37:121–140.

Silverstein, K. A. T., A. D. J. Haymet, and K. A. Dill. 1998. A simple model of water and the hydrophobic effect. *J. Am. Chem. Soc.* 120: 3166–3175.

Smith, P. E. 1999. Computer simulation of cosolvent effects on hydrophobic hydration. *J. Phys. Chem. B.* 103:525–534.

Sokolowski, S., and J. Fischer. 1990. Classical multicomponent fluid structure near solid substrates: Born-Green-Yvon equation versus density-functional theory. *Mol. Phys.* 70:1097–1113.

Sprous, D., M. A. Young, and D. L. Beveridge. 1998. Molecular dynamics studies of the conformational preferences of a DNA double helix in water and an ethanol/water mixture: theoretical considerations of the A $\Leftrightarrow$ B transition. *J. Phys. Chem. B.* 102:4658–4667.

Svergun, D. I., S. Richard, M. H. J. Koch, Z. Sayers, S. Kuprin, and G. Zaccai. 1998. Protein hydration in solution: experimental observation by x-ray and neutron scattering. *Proc. Natl. Acad. Sci. U.S.A.* 95: 2267–2272.

Tan, Z., U. Marini Bettolo Marconi, F. van Swol, and K. E. Gubbins. 1989. Hard-sphere mixtures near a hard wall. *J. Chem. Phys.* 90:3704–3712.

Tang, K. E. S., and V. A. Bloomfield. 2000. Excluded volume in solvation: sensitivity of scaled-particle theory to solvent size and density. *Biophys. J.* 79:2222–2234.

Throop, G. J., and R. J. Bearman. 1965. Radial distribution functions for mixtures of hard spheres. *J. Chem. Phys.* 42:2838–2843.

Throop, G. J., and R. J. Bearman. 1966. Radial distribution functions for binary fluid mixtures of Lennard-Jones molecules calculated from the Percus-Yevick equation. *J. Chem. Phys.* 44:1423–1444.

Timasheff, S. N. 1993. The control of protein stability and association by weak interactions with water: how do solvents affect these processes? *Annu. Rev. Biophys. Biomol. Struct.* 22:67–97.

Timasheff, S. N. 1998. Control of protein stability and reactions by weakly interacting cosolvents: the simplicity of the complicated. *Adv. Protein Chem.* 51:355–432.

Tirado-Rives, J., M. Orozco, and W. L. Jorgensen. 1997. Molecular dynamics simulations of the unfolding of barnase in water and 8 M aqueous urea. *Biochemistry* 36:7313–7329.

Vogler, E. A. 1998. Structure and reactivity of water at biomaterial surfaces. *Adv. Colloid Interface Sci.* 74:69–117.

Wüthrich, K., M. Billeter, P. Guntert, P. Luginbuhl, R. Riek, and G. Wider. 1996. NMR studies of the hydration of biological macromolecules. *Faraday Discussions.* 103:245–253.

Zhang, W., M. W. Capp, J. P. Bond, C. F. Anderson, and M. T. Record, Jr. 1996. Thermodynamic characterization of interactions of native bovine serum albumin with highly excluded (glycine betaine) and moderately accumulated (urea) solutes by a novel application of vapor pressure osmometry. *Biochemistry.* 35:10506–10516.